Direct laser writing-mediated generation of standardized topographies for dental implant surface optimization

Rainer Wittig[a),b)]
Institut für Lasertechnologien in der Medizin und Messtechnik (ILM) an der Universität Ulm, 89081 Ulm, Germany

Erik Waller[b)] and Georg von Freymann
Arbeitsgruppe Optische Technologien und Photonik und Forschungszentrum OPTIMAS, Fachbereich Physik, Technische Universität Kaiserslautern, 67663 Kaiserslautern, Germany

Rudolf Steiner
Institut für Lasertechnologien in der Medizin und Messtechnik (ILM) an der Universität Ulm, 89081 Ulm, Germany

(Received 14 October 2011; accepted for publication 18 May 2012; published 16 July 2012)

The functionalization of dental implants, aiming at the improvement of long-term acceptance, is of pivotal interest in dental research. Bone, connective tissue, and oral epithelium are in direct contact to the implant surface and exhibit distinct requirements for proper growth and differentiation. The authors applied direct laser writing and atomic layer deposition for the generation of TiO_2-coated micro and nanostructures which were subsequently tested for colonization and growth behavior of SaOs-2 cells, an osteosarcoma cell line revealing osteoblastic properties. Structures composed of rigid posts and flexible rods provide a matrix, which—when spaced adequately—favor the three-dimensional growth and proliferation of SaOs-2 cells. The results provide a proof of concept for the optimization of dental implant surfaces using generic techniques which deliver highly standardized structure motifs supporting the biological functions of the tissues affected. © *2012 Laser Institute of America*.

Key words: direct laser writing, dental implant, titanium dioxide, 3D scaffold, cell growth

I. INTRODUCTION

Dental implant complications represent a serious problem for the individuals concerned. Implant failure, leading to loss of the construct and the need for further dental prosthesis, occurs in approximately 5–8% of cases.[1] Major problems during implant adaptation to the body are (i) reduced formation of bone tissue, which impairs stable integration of the construct, (ii) parallel orientation of collagen fibers to the implant surface, which interferes with proper adhesion of connective tissue, and (iii) a lack of differentiation of epithelial cells, which inhibits a regular stratification of the oral epithelium and a tight junction between this tissue and the implant. These complications frequently lead to destabilization of the constructs and to periimplantitis and may successively result in dental implant loss.[2]

In the past, attempts for an optimization of the dental implant surface mainly focused on the interaction between titanium (as the material of choice for most constructs) and bone tissue. Modification of the titanium surface, e.g., by altering its hydrophilicity,[3] by providing integrin binding ligands or growth factor motifs,[4,5] by structural modifications,[6,7] or combinations of the latter[8,9] have been analyzed for an enhancement of cell growth, adhesion, and/or differentiation of osteoblasts, osteoblastlike cells, or mesenchymal stem cells. While such functionalizations frequently induced alterations in one of the parameters mentioned above, many of them have not been evaluated for an optimization of the balance between proliferation and differentiation, which is required for optimized osseointegration. A series of recent publications described elevated proliferation in line with osteogenic differentiation during growth of osteoblastlike cells on biphasic structural motifs composed of micro and nanostructures,[6,7] which was in part functionally validated by *in vivo* experiments.[10] The results suggest that a systematic analysis of cellular phenotypes during growth on titanium surfaces containing different biphasic structural motifs may facilitate the identification of further improvements on the way to an optimized osseointegration of dental implants.

The influence of substrate functionalization on soft tissues involved in dental implant adaptation has been studied with less intensity. Topography-dependent alterations in adhesion and signalling of gingival fibroblasts have been described.[11] *In vivo*, different implant surface structures affected the orientation of collagen fibers; however, the optimum perpendicular orientation was not observed in this study.[12] Growth factor coating of implants was found to alter the interaction between soft tissue and implant surface, but the orientation of fibroblasts and collagen fibers was not affected.[13]

Considering the precision required for the fabrication of tailored structures for proper differentiation of the affected tissues, rather arbitrary surface designs resulting from processes like acid-etching, machining, or sandblasting may be of minor quality and not sufficient for an optimal interaction

a)Electronic mail: rainer.wittig@ilm.uni-ulm.de
b)R. Wittig and E. Waller contributed equally to this work.

between cells and structures. To this end, we suggest direct laser writing (DLW) as a generic approach to produce highly standardized structures on dental implant surfaces, which meet the requirements of cell types under investigation. As a proof of concept, we generated structures which enabled three-dimensional growth and enhanced proliferation of osteoblastlike cells on titanium surfaces.

II. EXPERIMENTAL METHOD

A. Direct laser writing

Three-dimensional biphasic structures were created via two-photon absorption with a modified nanoscribe photonic professional direct laser writing system (Nanoscribe GmbH, Eggenstein-Leopoldshafen, Germany). The system is based on a 100 MHz pulsed erbium-doped and frequency doubled femtosecond fiber laser in the near infrared wavelength range (pulse duration 150 fs at 780 nm) as a light source, an acousto-optical device modulating the intensity, an inverted microscope for high numerical aperture focussing (numerical aperture NA = 1.4, oil-immersion), a three-axis piezo-electrical device for accurate motion of the sample (PhysikInstrumente), and a motorized stage for large-area coarse structuring [Fig. 1(a)]. Used photoresists include negative resists IP-L and IP-G (both commercially available from Nanoscribe). IP-L is dropcast onto a glass slide and developed by immersion in isopropanol for 20 min. IP-G is dropcast or spin-coated onto a glass slide and prebaked for 1 h at 100 °C. Development is performed by immersion in 1-methoxypropan-2-yl acetate for 20 min. No postbake is required. Typical laser power for writing the structures is in the range of 10–20 mW, measured at the entrance pupil of the objective. The writing speed for the structures was set to nominal 100 μm/s, but varies with the complexity of the structures.

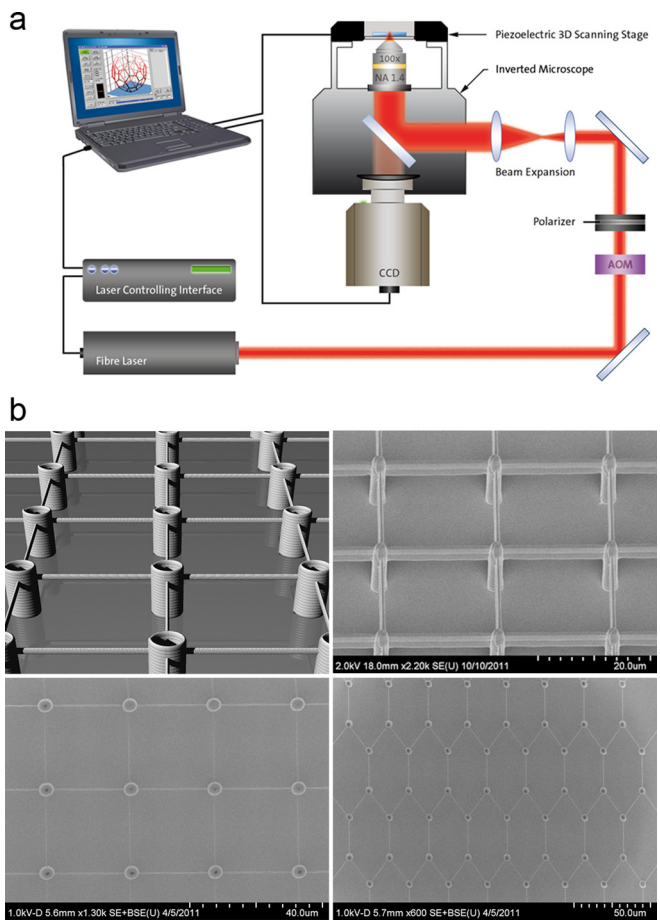

FIG. 1. Direct laser writing mediated generation of micro and nanostructures. (a) Optical setup for direct laser writing. (b) Schematic illustration of structures composed of rigid posts and flexible rods (upper left image) as well as exemplary SEM images of square and honeycomblike structures (upper right image: square, lateral view; lower left image: square, top view; lower right image: honeycomb, top view; post distance: 25 μm), which differ by post arrangement.

B. Atomic layer deposition (ALD)

After the lithography step and the development of the samples, ALD is used to coat the three-dimensional structures with 50 nm TiO_2 (anatase phase) to ensure biofunctionality and to provide photo-toxicity under illumination with UV-light. The ALD process is the only process that allows truly homogeneous film growth on three-dimensional structures since it is not a directed process. The coating is performed with a Cambridge Savannah system with 1667 cycles at 250 °C. Precursors were tetrakis(dimethylamino)titanium and H_2O.

C. Scanning electron microscopy (SEM)

SEM images were taken with a Hitachi SU-8000. The structures were not additionally coated.

D. Cell culture and proliferation analysis

SaOs-2 cells were kindly provided by Prof. Ignatius (Institut für Unfallchirurgische Forschung und Biomechanik, Ulm University). The cells were cultured in DMEM-medium containing 10% fetal calf serum, 100 U/ml penicillin, and 100 μg/ml streptomycin. For fluorescence imaging, cells were seeded at a density of 100 cells/mm^2 and grown for 48 h. Cell proliferation of structured and neighboring plain fields (1 mm^2 each) was determined by counting of 4′,6-diamidino-2-phenylindole (DAPI) stained nuclei 48 h post cell seeding. Two–three fields per structure were counted; the data represent mean values ± standard deviation.

E. Cell staining and fluorescence microscopy

Prior to staining, cells were fixed in phosphate buffered saline containing 4% formaldehyde. Vinculin staining for visualization of focal adhesion contacts (FACs) was carried out using a mouse monoclonal anti vinculin antibody (ab18058/clone SPM227, Abcam, Cambridge, UK) and an Alexa 488-conjugated goat antimouse secondary antibody (A11029, Invitrogen, Darmstadt, Germany). Actin microfilaments were visualized using phalloidin-tetramethylrhodamine isothiocyanate (Sigma-Aldrich, Taufkirchen, Germany). Nuclear staining was performed using DAPI (Sigma-Aldrich). Fluorescence microscopy was carried out using Zeiss microscopes (Axiovert 40CFL and LSM510) and software (AxioVision Rel. 4.8 and LSM5). Cell areas were determined by an implemented algorithm in the AxioVision software.

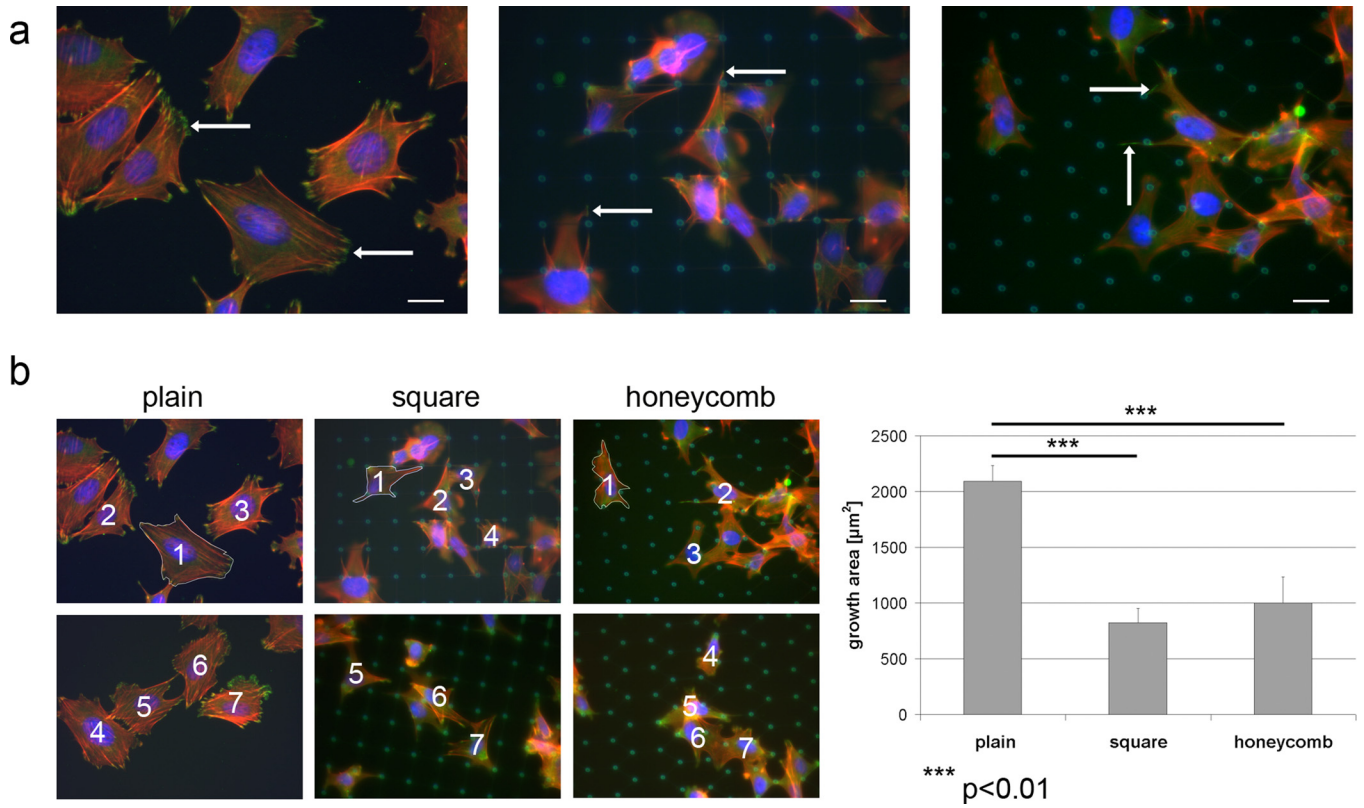

FIG. 2. SaOs-2 cell growth on titanium surfaces featuring different topographies. (a) Three colour fluorescence imaging (nuclei: blue; microfilaments: red; vinculin-stained FAC: green, exemplarily marked by white arrows) revealed large, flattened appearance and distinct focal adhesion contacts during two-dimensional growth of cells on plain surfaces (left image), whereas square (middle image) and honeycomb (right image) structures induced the formation of focal adhesion contacts at posts and rods of the structures, thus allowed cell growth in three dimensions (scale bar: 20 μm). (b) Growth areas occupied by cells were significantly reduced during three-dimensional growth. For each topography under investigation, seven cells (numbered 1–7 in the micrographs) were selected for the determination of growth areas using an area determination tool implemented in the AxioVision software. Growth area of cell #1 is exemplarily marked by a white borderline, respectively. Values are median ± median absolute deviation; significance was calculated using two-tailed student's t-test.

III. RESULTS

A. Generation of structures with varying feature sizes

Test structures were composed of rigid posts (5 μm diameter, 13 μm height) connected by thinner and thus more flexible rods [elliptical shape, long axis 780 nm, short axis 300 nm, distance from substrate 10 μm, see Fig. 1(b)]. The posts were arranged in either a square pattern or a honeycomblike pattern. The distance between posts has been varied between 10 and 50 μm in 10 μm steps for square patterns. In addition, honeycomb patterns and square patterns with 25 μm post distance were created alongside for comparison. Each sample contained three square fields of 1×1 mm^2 size for each structure type. The rigid posts have been written with piezopositioning, the connecting mesh of thinner rods with the motorized stage of the lithography system.

B. Three-dimensional growth of SaOs-2 cells in square and honeycomb structures

Fluorescence staining of microfilaments and FAC (via FAC bound vinculin) revealed a three-dimensional growth of cells in both square and honeycomb structures, which was evident through the identification of cytoplasmic protrusions touching posts and rods via FAC. In contrast cells on plain, unstructured areas revealed a flattened appearance and formed FAC at the basolateral side in contact with the titanium coated surface [Fig. 2(a)—scale bar is 20 μm; FACs are marked by white arrows]. When defined through presence of fluorescence signals from the cytoskeleton and FAC during epifluorescence microscopy, the growth area of cells in both square and honeycomb structures was significantly smaller when compared to plain surfaces [Fig. 2(b)].

C. SaOs-2 cell growth is enhanced in defined structure shapes and sizes

To investigate the influence of motif size on proliferation of SaOs-2 cells, coverslips featuring square structures providing post distances which varied between 10–50 μm were utilized. 48 h post seeding, cells were fixed and nuclei were stained with DAPI and counted on an area of 1 mm^2 for both structured and plain surfaces. Whereas a post distance of 10 μm led to reduced numbers of cells, we found elevated numbers of cells at a post distance of 25 μm. Post distances of 30 μm and larger did not seem to influence the proliferation of SaOs-2 cells (Fig. 3).

IV. DISCUSSION

In this study, direct laser writing combined with atomic layer deposition was successfully applied for the generation of TiO_2-coated structures at the micro and nanometer scale, which were subsequently analyzed for biocompatibility.

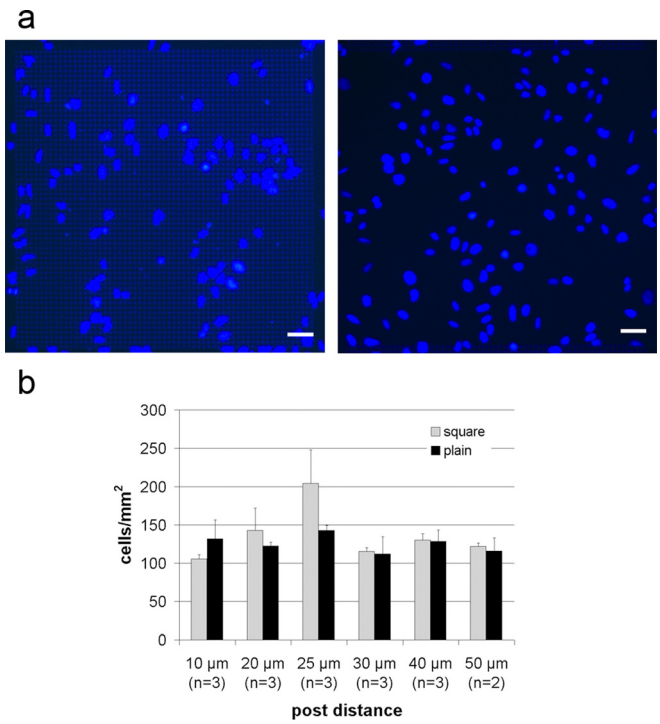

FIG. 3. Feature size influences proliferation of SaOs-2 cells. Cells were seeded on coverslips containing square motifs (compare Fig. 1) featuring different post distances and analyzed for proliferation 48 h post seeding. DAPI staining of nuclei and counting of cells on structured and neighboring plain areas was performed (1 mm^2 size, two—three experimental groups, respectively). Structures providing post distances of 10 μm tended to inhibit proliferation; structures providing 25 μm post distance tended to enhance proliferation. (a) Exemplary images of DAPI-stained cell nuclei on structures featuring 10 μm post distance (left) and corresponding plain area (right) (scale bar: 50 μm). (b) Quantitative analysis: values are mean ± standard deviation.

When spaced adequately, posts and rods provide a designer matrix which tends to enhance proliferation and enables three-dimensional growth of osteoblastlike cells. Our approach is applicable to rapidly generate highly standardized motifs in a controllable manner, thereby allowing for high-throughput screening of structural features which may facilitate implant acceptance. Thus, it offers the potential to establish a classification scheme of surface features, which is desired in the scientific community and could significantly improve implant biocompatibility.[14,15]

In general, titanium is well accepted by the organism.[16] Thus, the metal serves as a basic material for implants fulfilling different functions within the body, among them dental implants. The modification of titanium surfaces represents a frequently used approach for the optimization of implant biocompatibility. In the majority of cases, variations are of biochemical and/or physicochemical nature and include the binding of bioactive signal molecules[5] as well as modulations of surface hydrophilicity[3] or structure.[10] In most approaches, structural modifications are generated by physical or chemical impacts (e.g., sandblasting or etching), the results of which can be adjusted by altering process parameters, but, however, may be regarded as unorganized or not completely controllable in detail.[15,17] As a consequence, the variability of structures generated by these techniques is manifold. However, surface types are difficult to categorize, and a systematic analysis of the impact of variations in structural parameters on cellular growth, adhesion, and differentiation is incomplete and requires further investigation. Biphasic structures, as generated by acid-etching of surfaces and subsequent sputter-mediated deposition of TiO_2 nanonodules, were found to improve dental implant osseointegration, but also to impair biological functions of fibroblasts.[6] These results underline (i) the need for an identification of optimized structures for all tissues affected during dental implant acceptance and (ii) the importance of spatially resolved surface structuring, which assures the presence of an optimized micro-environment for each tissue affected. In this study, we provide evidence for the regulation of proliferative activity of osteoblast-like cells by the presence and size of highly ordered 3D structural motifs at the micrometer scale. In addition, the formation of FAC at both lateral and apical structural elements and a reduction of the growth area occupied suggest that our matrix provides a scaffold which is well accepted for 3D growth by osteoblast (-like) cells. The differentiation-promoting effects of three-dimensional growth of osteoblast (-like) cells induced by the presence of artificial 3D scaffolds have been demonstrated by others.[18–20] Since proper osteogenesis requires a delicate balance between proliferation and differentiation, further studies are needed to analyze the influence of our scaffolds on hallmarks of osteoblast differentiation, such as alkaline phosphatase activity, osteocalcin secretion, or hydroxyapatite deposition.

The requirement for precision of features at the nanometer scale for biological applications has been demonstrated.[21,22] Regular spacing of features and the degree of flexibility of the micro-environment (determining mechanically induced signal transduction in target cells) have profound impact on physiology of various cell types, thus justifying research on designer extracellular matrices for medical applications.[23] Direct laser writing has already been successfully employed for the controlled generation and functionalization of 3D structures for biological applications at the submicrometer scale. Photoresists such as ORMOCER and SU8 have been proven for their biocompatibility,[24] and 3D structures generated have been demonstrated to support the development of characteristic phenotypes for a variety of cell types, among them granulosa cells, fibroblasts, chondrocytes as well as endothelial, epithelial, and cancer cells.[25–27] Recent research of our lab addressed the impact of structure flexibility and scaffold functionalization on cellular properties.[28,29] However, the method lacked the potential for structuring areas of sufficient size and sub-100 nm resolution.

To this end, we combined stage- and piezo-electrical scanning to fabricate structures covering areas up to 1 cm^2. Within this, the creation of sub-100 nm features and minimum feature separations down to 300 nm have been targeted and achieved by the development of new photoresists,[30] which have been thoroughly characterized for two-photon polymerization by femtosecond laser pulses and were also shown to be suited for two-photon polymerization using continuous-wave (cw) diode lasers at wavelengths down to 532 nm.[31]

While the present work focuses on the influence of large-area structures with submicron feature sizes on osteoblast-like cells, the new photoresists should enable the generation of well-defined biphasic structures containing precise details at the sub-100 nm scale for future

applications. Further progress in structuring of crooked surfaces should then facilitate the generation of tailored topographical features for an optimized interaction of dental implants with both hard and soft tissues.

ACKNOWLEDGMENTS

This study was supported by a grant from the German Research Foundation (STE490/23-1 to R.S. and FR1671/6-1 to G.v.F.). The authors thank Eva Winkler and Petra Kruse for expert technical assistance, Andreas Frölich for running part of the atomic-layer coatings, and Herbert Schneckenburger and his group for valuable support in fluorescence microscopy. G.v.F. is cofounder of Nanoscribe GmbH, commercializing direct laser writing and corresponding photoresist materials.

[1]P. K. Moy, D. Medina, V. Shetty, and T. L. Aghaloo, "Dental implant failure rates and associated risk factors," Int. J. Oral Maxillofac Implants **20**, 569–577 (2005).
[2]S. Sakka and P. Coulthard, "Implant failure: Etiology and complications," Med. Oral Patol. Oral Cir. Bucal. **16**, e42–e44 (2011).
[3]G. Zhao, Z. Schwartz, M. Wieland, F. Rupp, J. Geis-Gerstorfer, D. L. Cochran, and B. D. Boyan, "High surface energy enhances cell response to titanium substrate microstructure," J. Biomed. Mater. Res. Part A **74**, 49–58 (2005).
[4]B. F. Bell, M. Schuler, S. Tosatti, M. Textor, Z. Schwartz, and B. D. Boyan, "Osteoblast response to titanium surfaces functionalized with extracellular matrix peptide biomimetics," Clin. Oral Implants Res. **22**, 865–872 (2011).
[5]Y. J. Seol *et al.*, "Enhanced osteogenic promotion around dental implants with synthetic binding motif mimicking bone morphogenetic protein (BMP)-2," J. Biomed. Mater. Res. Part A **77**, 599–607 (2006).
[6]N. Hori *et al.*, "Selective cell affinity of biomimetic micro-nano-hybrid structured TiO_2 overcomes the biological dilemma of osteoblasts," Dent. Mater. **26**, 275–287 (2010).
[7]R. A. Gittens *et al.*, "The effects of combined micron-/submicron-scale surface roughness and nanoscale features on cell proliferation and differentiation," Biomaterials **32**, 3395–3403 (2011).
[8]G. Balasundaram, C. Yao, and T. J. Webster, "TiO_2 nanotubes functionalized with regions of bone morphogenetic protein-2 increases osteoblast adhesion," J. Biomed. Mater. Res. Part A **84**, 447–453 (2008).
[9]L. Zhang, U. D. Hemraz, H. Fenniri, and T. J. Webster, "Tuning cell adhesion on titanium with osteogenic rosette nanotubes," J. Biomed. Mater. Res. Part A **95**, 550–563 (2010).
[10]K. Kubo, N. Tsukimura, F. Iwasa, T. Ueno, L. Saruwatari, H. Aita, W. A. Chiou, and T. Ogawa, "Cellular behavior on TiO_2 nanonodular structures in a micro-to-nanoscale hierarchy model," Biomaterials **30**, 5319–5329 (2009).
[11]E. Kokubu, D. W. Hamilton, T. Inoue, and D. M. Brunette, "Modulation of human gingival fibroblast adhesion, morphology, tyrosine phosphorylation, and ERK 1/2 localization on polished, grooved and SLA substratum topographies," J. Biomed. Mater. Res. Part A **91**, 663–670 (2009).
[12]S. Yamano, Z. H. Al-Sowygh, G. O. Gallucci, K. Wada, H. P. Weber, and C. Sukotjo, "Early peri-implant tissue reactions on different titanium surface topographies," Clin. Oral Implants Res. **22**, 815–819 (2011).
[13]C. Bates, V. Marino, N. L. Fazzalari, and M. Bartold, "Soft tissue attachment to titanium implants coated with growth factors," Clin. Implant Dent. Relat. Res. doi: 10.1111/j.1708-8208.2010.00327.x (2011).
[14]M. Bächle and R. J. Kohal, "A systematic review of the influence of different titanium surfaces on proliferation, differentiation and protein synthesis of osteoblast-like MG63 cells," Clin. Oral Implants Res. **15**, 683–692 (2004).
[15]D. M. Dohan Ehrenfest, P. G. Coelho, B. S. Kang, Y. T. Sul, and T. Albrektsson, "Classification of osseointegrated implant surfaces: Materials, chemistry and topography," Trends Biotechnol. **28**, 198–206 (2010).
[16]D. M. Brunette, P. Tengvall, M. Textor, and P. Thomsen, in *Titanium in Medicine: Material Science, Surface Science, Engineering, Biological Responses and Medical Applications*, edited by D. M. Brunette (Springer-Verlag, Berlin, 2001).
[17]G. Mendonça, D. B. Mendonça, F. J. Aragão, and L. F. Cooper, "Advancing dental implant surface technology—From micron- to nanotopography," Biomaterials **29**, 3822–3835 (2008).
[18]D. Ferrera *et al.*, "Three-dimensional cultures of normal human osteoblasts: Proliferation and differentiation potential *in vitro* and upon ectopic implantation in nude mice," Bone **30**, 718–725 (2002).
[19]M. J. Dalby, N. Gadegaard, R. Tare, A. Andar, M. O. Riehle, P. Herzyk, C. D. Wilkinson, and R. O. Oreffo, "The control of human mesenchymal cell differentiation using nanoscale symmetry and disorder," Nature Mater. **6**, 997–1003 (2007).
[20]I. K. Shim, M. R. Jung, K. H. Kim, Y. J. Seol, Y. J. Park, W. H. Park, and S. J. Lee, "Novel three-dimensional scaffolds of poly(L-lactic acid) microfibers using electrospinning and mechanical expansion: Fabrication and bone regeneration," J. Biomed. Mater. Res., B: Appl. Biomater. **95**, 150–160 (2010).
[21]M. Arnold, E. A. Cavalcanti-Adam, R. Glass, J. Blümmel, W. Eck, M. Kantlehner, H. Kessler, and J. P. Spatz, "Activation of integrin function by nanopatterned adhesive interfaces," ChemPhysChem. **5**, 383–388 (2004).
[22]E. A. Cavalcanti-Adam, T. Volberg, A. Micoulet, H. Kessler, B. Geiger, and J. P. Spatz, "Cell spreading and focal adhesion dynamics are regulated by spacing of integrin ligands," Biophys. J. **92**, 2964–2974 (2007).
[23]B. Geiger, J. P. Spatz, and A. D. Bershadsky, "Environmental sensing through focal adhesions," Nat. Rev. Mol. Cell Biol. **10**, 21–33 (2009).
[24]A. Ovsianikov, S. Schlie, A. Ngezahayo, A. Haverich, and B. N. Chichkov, "Two-photon polymerization technique for microfabrication of CAD-designed 3D scaffolds from commercially available photosensitive materials," J. Tissue Eng. Regener. Med. **1**, 443–449 (2007).
[25]A. Koroleva *et al.*, "Microreplication of laser-fabricated surface and three-dimensional structures," J. Opt. **12**, 124009 (2010).
[26]P. Tayala, C. R. Mendonca, T. Baldacchini, D. J. Mooney, and E. Mazur, "3D cell-migration studies using two-photon engineered polymer scaffolds," Adv. Mater. **20**, 4494–4498 (2008).
[27]T. Weiß, R. Schade, T. Laube, A. Berg, G. Hildebrand, R. Wyrwa, M. Schnabelrauch, and K. Liefeith, "Two-photon polymerization of biocompatible photopolymers for microstructured 3D biointerfaces," Adv. Eng. Mater. **13**, B264–B273 (2011).
[28]F. Klein, T. Striebel, J. Fischer, Z. Jiang, C. M. Franz, G. von Freymann, M. Wegener, and M. Bastmeyer, "Elastic fully three-dimensional microstructure scaffolds for cell force measurements," Adv. Mater. **22**, 868–871 (2010).
[29]F. Klein, B. Richter, T. Striebel, C. M. Franz, G. von Freymann, M. Wegener, and M. Bastmeyer, "Two-component polymer scaffolds for controlled three-dimensional cell culture," Adv. Mater. **23**, 1341–1345 (2011).
[30]M. Thiel, "Design, fabrication and characterization of three-dimensional chiral photonic crystals," PhD thesis, Institute of Applied Physics, Karlsruhe Institute of Technology (KIT), 2010.
[31]M. Thiel, J. Fischer, G. von Freymann, and M. Wegener, "Direct laser writing of three-dimensional sub-micron structures using a continuous-wave laser at 532 nm," Appl. Phys. Lett. **97**, 221102 (2010).